

See discussions, stats, and author profiles for this publication at: <https://www.researchgate.net/publication/273386926>

Structural, Thermal and Anti-inflammatory Properties of A Novel Pectic Polysaccharide from Alfalfa (*Medicago sativa L.*) Stem.

ARTICLE in JOURNAL OF AGRICULTURAL AND FOOD CHEMISTRY · MARCH 2015

Impact Factor: 2.91 · DOI: 10.1021/acs.jafc.5b00494 · Source: PubMed

CITATIONS

3

READS

92

6 AUTHORS, INCLUDING:



Lei Chen

Chinese Academy of Sciences

17 PUBLICATIONS 71 CITATIONS

[SEE PROFILE](#)



Bona Dai

Shanghai Jiao Tong University

8 PUBLICATIONS 26 CITATIONS

[SEE PROFILE](#)



Liangli Lucy Yu

University of Maryland, College Park

155 PUBLICATIONS 5,083 CITATIONS

[SEE PROFILE](#)

Structural, Thermal, and Anti-inflammatory Properties of a Novel Pectic Polysaccharide from Alfalfa (*Medicago sativa* L.) Stem

Lei Chen,[†] Jie Liu,[†] Yaqiong Zhang,[†] Bona Dai,[‡] Yuan An,[#] and Liangli (Lucy) Yu*,^{†,§}

[†]Institute of Food and Nutraceutical Science, School of Agriculture and Biology, [‡]Instrumental Analysis Center, and [#]School of Agriculture and Biology, Shanghai Jiao Tong University, Shanghai 200240, China

[§]Department of Nutrition and Food Science, University of Maryland, College Park, Maryland 20742, United States

Supporting Information

ABSTRACT: A pectic polysaccharide (APPS) was purified from the cold alkali extract of alfalfa stem and characterized to be a rhamnogalacturonan I (RG-I) type pectin with the molecular weight of 2.38×10^3 kDa and a radius of 123 nm. The primary structural analysis indicated that APPS composed of a $\rightarrow 2$ - α -L-Rhap-(1 \rightarrow 4)- α -D-GalpA-(1 \rightarrow) backbone with 12% branching point at C-4 of Rhap forming side chains by L-arabinosyl and D-galactosyl oligosaccharide units. Transmission electron microscopy (TEM) analysis revealed a primary linear-shaped structure with a few branches in its assembly microstructures. The thermal decomposition evaluation revealed the stability of APPS with an apparent activation energy (E_a) of 226.5 kJ/mol and a pre-exponential factor (A) of 2.10×10^{25} /s, whereas its primary degradation occurred in the temperature range from 215.6 to 328.0 °C. In addition, APPS showed significant anti-inflammatory effect against mRNA expressions of the pro-inflammatory cytokine genes, especially for IL-1 β , suggesting its potential utilization in functional foods and dietary supplement products.

KEYWORDS: *alfalfa pectic polysaccharide, rhamnogalacturonan I, thermal analysis, anti-inflammatory effect*

INTRODUCTION

Alfalfa (*Medicago sativa* L.), so-called “king of forages”, has been cultivated as an important perennial forage crop worldwide.¹ Alfalfa is mainly used as a livestock feed for its high content of crude protein and excellent quality of vitamins and minerals.² Meanwhile, the dietary fiber content of alfalfa is also high but usually ignored. In the 1960s, alfalfa was reported to contain two types of noncellulosic polysaccharides, including hemicellulose and pectin.^{3,4} There have been several reports about the monosaccharide composition and linkage types of pectic polysaccharides from alfalfa stems and leaves since the 1960s’, but little is known about the fine structure of alfalfa pectic polysaccharides.^{4,5} Also, bioactivity of alfalfa polysaccharides in immune modulation, antioxidant, and anticancer has been reported, but the details for their structures and thermal properties have not been investigated.^{6–8} This situation significantly restricts the further development and application of value-added utilization of alfalfa in other fields including the materials, energy, medical, and food industries.

Pectins, also known as pectic polysaccharides, are some of the most abundant structural components of plant cell walls. The types and contents of pectin vary largely on the basis of their plant sources and growth stages. In general, pectins contain an acidic backbone of homogalacturonan and/or rhamnogalacturonan with different types of neutral side chains commonly composed of arabinose, galactose, and xylose.^{9,10} They are classified as a family of complex polysaccharides containing 1,4-linked D-galacturonic acid (GalpA) residues and are usually divided into homogalacturonans (HG), rhamnogalacturonan I (RG-I), rhamnogalacturonan II (RG-II), xylogalacturonan (XGA), and apiogalacturonan (AGA) on the basis of their structural features.^{11,12} Compared with hemicellulose, pectin is mostly water-soluble and widely applied in some

important fields, including the pharmaceutical, cosmetics, and food industries, for their unique properties, such as textural food ingredients or gelling and thickening agents.^{13–15} Besides, on the basis of their potential bioactivities, the utility of these polysaccharides as functional foods is increasingly recognized.^{13,14} Therefore, it is necessary to investigate the exact architecture of pectins, which remains disputed.¹⁶

Texture degradation has been evaluated as an important property of pectin by thermal decomposition analysis.^{17,18} The thermal decomposition analysis has been conducted for several natural fibers including cellulose, hemicellulose, lignin and isolated pure polysaccharides.^{19,20} Thermal analysis was also widely applied in the food industry, including the determination of gelatinization temperature and enthalpy of starch,²¹ the thermal stability of foods and their composites, such as oil and protein,^{22,23} and the reaction between food components.²⁴ Thermal analysis of polysaccharides is an important evaluation for their stability and shelf life in further application for the food industry.

In this study, we demonstrate the fine structure and molecular morphology of a pectic polysaccharide purified from alfalfa stem. Moreover, the thermal decomposition characteristics and anti-inflammatory effect of this polysaccharide were also evaluated for further development of its potential food applications. To our knowledge, this is the first time that thermal decomposition analysis and in vitro anti-inflammatory determination were performed on a purified pectic polysaccharide from alfalfa stem.

Received: January 26, 2015

Revised: March 8, 2015

Accepted: March 10, 2015

Published: March 10, 2015

MATERIALS AND METHODS

Materials. The alfalfa sample was harvested in the time period between the bud and initial flowering stage (10% bloom) from Gansu province of China and dried at environmental conditions. TRIzol reagent was purchased from Invitrogen (Carlsbad, CA, USA), whereas an iScript Advanced cDNA Synthesis kit was purchased from Bio-Rad (Hercules, CA, USA). RAW 264.7 mouse macrophage cells were obtained from the Chinese Academy of Sciences (Shanghai, China). Lipopolysaccharide (LPS) from *Escherichia coli* O111:B4 was obtained from Millipore (Bedford, MA, USA). Other reagents for isolation were of analytical grade without further purification.

Fractionation and Purification of Pectic Polysaccharide. After removal of the leaves, the dried alfalfa stem was milled into powders through a 200-mesh screen using an IKA mill (IKA, A11, Germany). Small molecules were removed from alfalfa stem powders by three 95% ethanol extractions at 75 °C for 2 h. Afterward, hot water (DD H₂O, 80 °C, 2 h; three times) and cold alkali (1 M NaOH, room temperature, 12 h; four times) were successively used to extract the water-soluble substances and hemicellulosic polysaccharides (Figure S1). The pectins were then extracted four times using a 20-fold volume of 1 M NaOH (w/v) at 80 °C with continuous stirring for 2 h. After neutralization with HCl solution, the extract was precipitated by using a 4-fold volume of 95% ethanol (v/v) and washed three times with 75% ethanol, followed by lyophilization to afford the crude pectic polysaccharides of alfalfa stem.

Further purification was carried out by membrane ultrafiltration (Minimate TFF system, Pall Corp., Port Washington, NY, USA) with defined exclusion limits of 10000 Da to obtain the pectic polysaccharide molecules of alfalfa stem (APPS) with MW >10000 Da. The cutoff polysaccharide was then purified by gel filtration chromatography on a Sephadex S-400 Superfine column (80 × 1.6 cm i.d., Amersham Pharmacia Biotech, Uppsala, Sweden) eluted with DD H₂O at 1.0 mL/min. The collected eluates were combined and freeze-dried prior to further analysis (Figure S1).

Molecular Weight and Size Determination. The molecular weight and size of APPS were determined using a particle size analyzer (Zetasizer Nano-ZS90, Malvern Instruments Ltd., Malvern, Worcs, UK). In general, the well-dispersed APPS stock aqueous solution (2 mg/mL) was diluted to 1.00, 0.75, 0.50, 0.25, and 0.10 mg/mL. The Debye plot from static light scattering (SLS) was obtained to calculate the weight-averaged molecular weight (M_w) of APPS based on the Rayleigh equation (eq 1).²⁵

$$\frac{KC}{R_\theta} = \left(\frac{1}{M_w} + 2A_2 C \right) \times P(\theta) \quad (1)$$

In eq 1, K , M_w , A_2 , C , and R_θ represent optical constant, sample molecular weight, second virial coefficient, concentration, and Rayleigh ratio, respectively. Representing the angular dependence of the sample scattering intensity, the value of $P(\theta)$ would reduce to 1 when the particles are much smaller than the wavelength of the incident light. The M_w (Da or g/mol) was determined from the intercept at zero concentration ($C \rightarrow 0$) according to $KC/R_\theta = 1/M_w$. The molecular size was simultaneously obtained along with the molecular weight determination at the concentration of 0.25 mg/mL.

Chemical Composition Analysis. APPS was analyzed for contents of total protein, carbohydrate, and uronic acid using bicinchoninic acid (BCA),²⁶ phenol–sulfuric acid,²⁷ and *m*-hydroxydiphenylsulfuric acid²⁸ methods, respectively.

The PMP derivation method was used to determine the monosaccharide and uronic acid compositions of APPS as described previously.²⁹ The obtained sugar derivatives were then determined by HPLC analysis at 250 nm with an Inertsil ODS-3 column (100 mm × 2.1 mm i.d., 2 μm, GL Sciences Inc., Tokyo, Japan) under the following chromatographic conditions: 30 °C, 0.1 M phosphate buffer (pH 6.7)/acetonitrile at a ratio of 80:20 (v/v), 0.3 mL/min.

Linkage Analysis by Methylation. APPS was first reacted with NaBD₄ to reduce the uronic acid residues according to a previously reported protocol.³⁰ The partially methylated alditol acetates (PMAAs) of APPS was prepared according to a modified Needs

method³¹ for the following determination using GC-MS (Agilent 7890A-5975C, Agilent Technology, Santa Clara, CA, USA), equipped with a HP-5 capillary column (30 m × 0.32 mm i.d., 0.25 μm film). The temperature of GC was increased from 50 to 150 °C at 30 °C/min, then to 220 °C at 3 °C/min, and finally to 300 °C at 30 °C/min and held for 10 min. The injector temperature was set at 250 °C, whereas the interface temperature was 280 °C. The MS parameters were set as ion source temperature at 300 °C, ionization energy at 70 eV, detector voltage at 1.5 kV, and mass range from 50 to 550. Glycosidic linkages of APPS were identified by comparing the mass spectrum patterns of PMAAs with the database of CCRC.³² The molar ratios of individual linkage residues were calculated on the basis of peak areas and response factors for each sugar in the TIC as described previously.³³

Spectroscopic Analysis. The infrared spectrum of APPS was measured on a FT-IR spectrometer (Nicolet 6700, Thermo Fisher, Waltham, MA, USA) using KBr pellets in the infrared region of 4000–400 cm⁻¹ at a resolution of 4 cm⁻¹. One- and two-dimensional NMR analyses of APPS were carried out on an Avance Bruker III HD 600 MHz NMR spectrometer equipped with a 5 mm TCI CryoProbe at 25 °C using D₂O as the solvent to a final sample concentration of 40 mg/mL.

Transmission Electron Microscopy (TEM). In brief, a well-dispersed polysaccharide solution was first prepared using sodium dodecyl sulfate (SDS, 5 μg/mL) to a final concentration of 5 μg/mL. SDS aqueous solution was applied to dissolve APPS as the SDS solution could reduce the molecular aggregation.³⁴ A droplet of APPS solution (5 μL) was deposited on a carbon film specimen (200 mesh, Beijing Zhongjingkeyi Technology, Beijing, China) and dried at ambient temperature and humidity. The specimen was examined using TEM (Tecnai G2 Spirit BIOTWIN, FEI, Hillsboro, OR, USA) at an accelerating voltage of 120 kV to observe the morphology of APPS molecular assembly or the microstructures of APPS.

Isoconversional Thermal Characteristics. Pyrolysis characteristics of APPS were determined on a simultaneous thermal analyzer (SDT-Q600, TA Instruments, New Castle, DE, USA). In general, three different heating rates (including 5, 10, and 20 °C/min) were used to decompose the APPS sample from 50 to 600 °C under N₂ protection at a flow rate of 100 cm³/min. The decomposition results were analyzed using the Flynn–Wall–Ozawa (FWO) method (eq 2) to obtain the experimental apparent activation energy (E_a).^{35–37}

$$\log \beta = \log \frac{AE_a}{Rg(\alpha)} - 2.315 - 0.4567 \frac{E_a}{RT} \quad (2)$$

where $g(\alpha) = \int_0^\alpha (da)/(f(a))$, β is the heating rate, R is the general gas constant, A stands for the pre-exponential factor, E_a is the apparent activation energy, and T is the temperature at the conversion α . The experimental value of ln A was obtained by the compensation effect relationship (eq 3), the compensation parameters (a and b) of which could be deduced by a plot of ln A versus E_a from a model-fitting approach using the Coats–Redfern equation (eq 4) with T' being the average experimental temperature.

$$\ln A = aE_a + b \quad (3)$$

$$\ln \frac{g(\alpha)}{T^2} = \ln \left[\left(\frac{AR}{\beta E_a} \right) \left(1 - \frac{2RT'}{E_a} \right) \right] - \frac{E_a}{RT} \quad (4)$$

Both the FWO and Coats–Redfern methods were classified to model-free methods. By using these methods, the process is detectable in the form of a dependence of the activation energy E_a on the conversion rate α . The thermal analysis data were analyzed using the Universal Analysis 2000 software (version 4.5A, TA Instruments) and MS Excel 2013.

Anti-inflammatory Bioactivity Determination. The potential anti-inflammatory effect of APPS was evaluated by determining its potential inhibition of IL-1β, IL-6, and COX-2 gene expressions in the cultured RAW 264.7 mouse macrophage cells. Briefly, the aqueous solution of APPS was first prepared at two different treatment concentrations (10 and 50 μg/mL). RAW 264.7 cells were cultured in

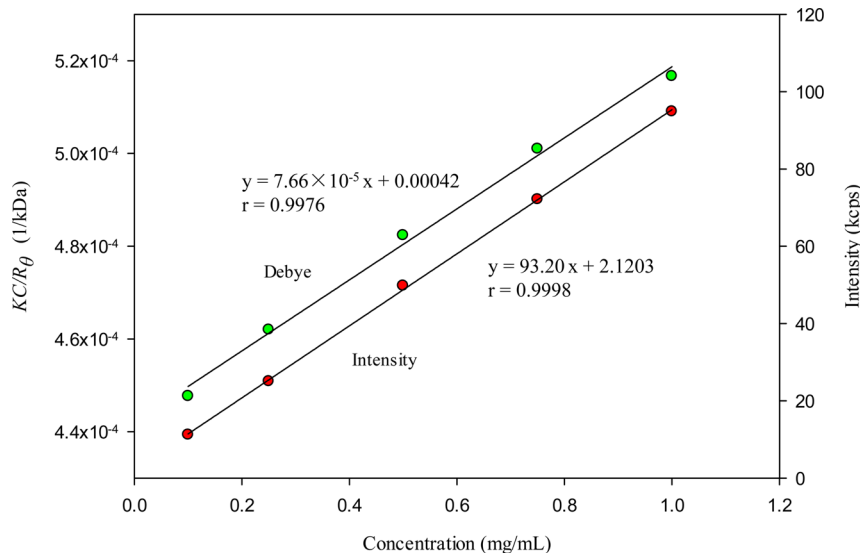


Figure 1. Debye plot of APPS for its molecular weight determination: angular dependences of KC/R_θ with K being the optical constant, C being the concentration, R_θ being the Rayleigh ratio, and θ being the scattering angle.

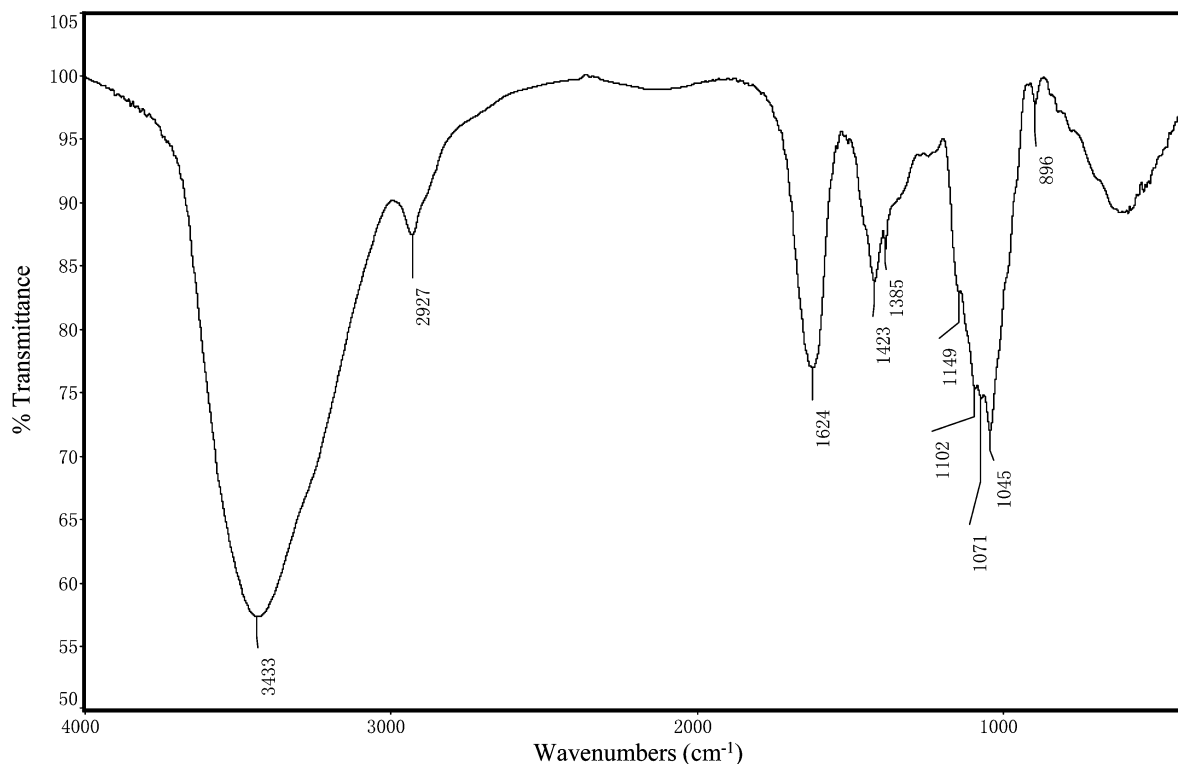


Figure 2. FT-IR spectrum of APPS.

6-well plates for 24 h to reach an 80% confluence before the treatment. After further incubation for 24 h, LPS was pipetted into the medium at a final concentration of 10 ng/mL and incubated for another 4 h at 37 °C under 5% CO₂.^{38,39} Total RNA was isolated from the mouse peritoneal macrophages using a TRIzol reagent (Invitrogen) for further reverse transcription of cDNA and real-time PCR analysis using the iScript Advanced cDNA Synthesis kit on an ABI 7900HT Fast Real-Time PCR System (Applied Biosystems) with the following PCR conditions: 50 °C for 2 min, 95 °C for 10 min, and 46 cycles of amplification at 95 °C for 15 s and 60 °C for 1 min.

Statistical Analysis. Data were recorded as the mean \pm SD for triplicate determination. The significance of differences between means were evaluated by one-way analysis of variance (ANOVA) and Tukey's

test using SPSS for Windows (version rel. 18.0, SPSS Inc., Chicago, IL, USA) with statistical significance assigned at $P < 0.05$.

RESULTS AND DISCUSSION

Preparation of APPS. The crude hot alkali extractable fraction was about 3.31% dry weight of the alfalfa stem and contained 96.79% (w/w) of total carbohydrate including 10.03% uronic acid, whereas no protein was detected. A homogeneous polysaccharide fraction was purified from the crude extract by ultrafiltration and size exclusion chromatography (SEC) and designated APPS (Figure S2). APPS

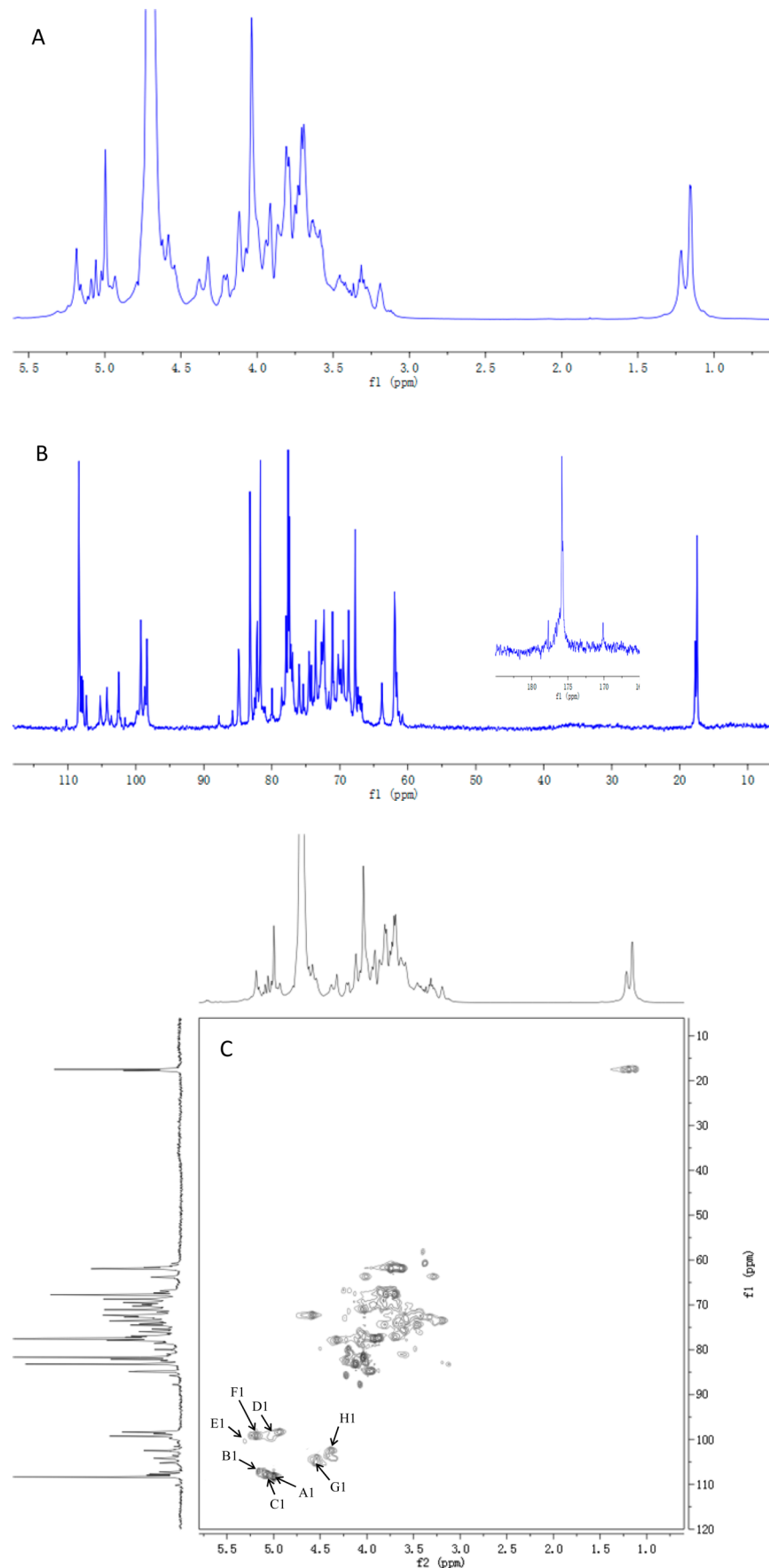


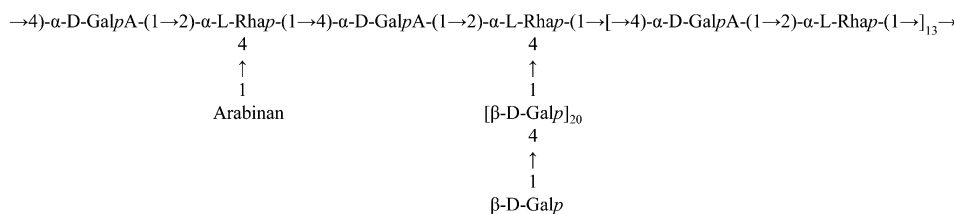
Figure 3. ^1H (A), ^{13}C (B), and HSQC (C) NMR spectra of APPS in D_2O solution at 25°C . A1 means the correlation between C1 and H1 of residue A. The order of residues A, B, C...H is consistent with Table 1.

Table 1. ^1H and ^{13}C NMR Chemical Shifts of APPS Recorded in D_2O at 25 °C^a

no.	residue	chemical shift, δ						
		1	2	3	4	5	6	COOH
A	$1,5\text{-}\alpha\text{-L-Araf}$	H	5.00	4.03	3.91	4.12	3.79, 3.69	
		C	106.81	81.75	79.01	83.11	67.62	
B	$T\text{-}\alpha\text{-L-Araf}$	H	5.16	4.17	3.86	4.22	4.01	
		C	107.09	80.87	78.39	85.71	63.64	
C	$1,3,5\text{-}\alpha\text{-L-Araf}$	H	5.06	4.04	3.86	3.96	3.74	
		C	107.83	79.93	84.68	84.84	67.55	
D	$1,2\text{-}\alpha\text{-L-Rhap}$	H	5.03	3.92	3.67	3.33	3.82	1.21
		C	98.56	77.53	70.67	72.71	69.08	17.45
E	$1,2,4\text{-}\alpha\text{-L-Rhap}$	H	5.31	4.20	4.03	3.99	3.71	1.25
		C	100.42	79.95	70.97	79.30	67.55	17.55
F	$1,4\text{-}\alpha\text{-D-GalpA}$	H	5.19	4.03	4.05	4.32	4.58	
		C	99.17	69.20	70.97	77.83	72.26	175.82
G	$1,4\text{-}\beta\text{-D-Galp}$	H	4.53	3.42	3.58	3.99	3.62	3.73
		C	102.31	72.47	73.04	79.30	75.43	61.81
H	$T\text{-}\beta\text{-D-Galp}$	H	4.38	3.18	3.47	3.70	3.62	3.64
		C	102.60	73.49	74.43	69.93	75.43	61.83

^aResidues A, B, C...H are designated according to the decreasing order of proton peak intensity.

A



B

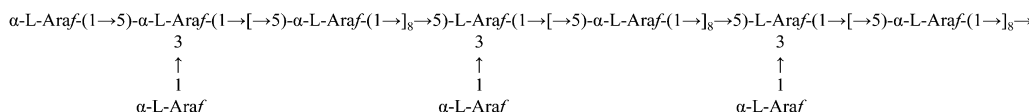


Figure 4. Proposed repeating units of APPS molecular structure: (A) schematic structure of APPS; (B) schematic structure of arabinan side chains in APPS.

consisted of rhamnose, galactose, galactouronic acid, and arabinose in a molar ratio of 2.4:1.4:1.0:3.4 (data not shown).

The M_w of APPS was calculated to be 2.38×10^3 kDa (or 2.38×10^6 g/mol) (Figure 1), whereas A_2 was calculated to be 7.66×10^{-5} from the gradient of the Debye plot, which indicated the aqueous solution of APPS was a stable system for the sake of A_2 over zero.⁴⁰ In addition, the average radius of APPS was simultaneously determined to be 123 nm.

Glycosidic Linkages of APPS. The result of PMAA analysis demonstrated that APPS was composed of eight different linkage residues including nonreducing terminals of arabinose ($T\text{-L-Araf}$) and galactose ($T\text{-D-Galp}$), the molar ratios of which are listed in Table S1 in the Supporting Information. The arabinose residues were primarily $1,5\text{-L-Araf}$, whereas the rhamnose residues were mainly $1,2\text{-L-rhamnose}$ (Rhap). Large percentages of $1,4\text{-D-Galp}$ and $1,4\text{-D-galactouronic acid}$ (GalpA) were also determined as the intrachain residues. The main branching points were at $1,3,5\text{-L-Araf}$ and $1,2,4\text{-L-Rhap}$. The ratio between terminal units and branching points was 0.97, indicating that the number of terminal units was approximately equal to the number of branching points in the polysaccharide.

Additionally, the degree of branching (DB) value was 12% for APPS according to the equation $DB = (NT + NB)/(NT + NB + NL)$,⁴¹ where NT, NB, and NL are the numbers of the terminal residues, branch residues, and linear residues, respectively.

FT-IR Spectrum. Figure 2 shows the primary maxima of absorption bands in IR spectra of APPS. The strong absorption at 3433 cm^{-1} was dominated by the stretching vibrations of OH, whereas the band at 2927 cm^{-1} was attributed to stretching vibrations of CH_3 . The signal at 1624 cm^{-1} was originated from the blending of water $\delta(\text{H}_2\text{O})$, indicating H–O–H angle vibration. The bands at 1423 and 1385 cm^{-1} were assigned to be carboxylate groups of APPS.⁴² Among them, the absorptions at 1624 and 1423 cm^{-1} were the characteristic peaks of pectin material, whereas no peak was detected at $\sim 1750 \text{ cm}^{-1}$, indicating the absence of carboxyl ester groups.⁴³ In the region of 1200 – 950 cm^{-1} , several intense signals at 1149 , 1102 , 1071 , and 1045 cm^{-1} contributed by the vibrations of glycosidic bonds and pyranoid rings.⁴³ Moreover, the band maximum at 1045 cm^{-1} was usually found in arabinogalacto-

rhamnoglycan, containing the dominant arabinose and rhamnose over the galactose units.⁴⁴

Structural Characterization by NMR Analysis. Linkages between glycosyl residues in APPS were further investigated by NMR analyses, including ¹H NMR, ¹³C NMR, and HSQC spectra (Figure 3), with the assistance of single-bond (COSY) and multiple-bond (TOCSY) proton–proton correlations (Figure S3). As shown in Figure 3C, eight cross peaks were presented in the anomeric region (¹H is from 4.3 to 5.5 ppm, whereas ¹³C is in the range of 90–120 ppm) of the HSQC spectrum. The chemical shift assignments of ¹H and their corresponding ¹³C were identified and are summarized in Table 1 from the above spectra according to the literature data for arabinofuranosides, arabinans, and pectins.^{45–47} The backbone was indicated by the presence of the characteristic C-1 signals (Figure 3B) of α -(1→4)-GalpA and α -(1→2)-Rhap at 99.17 and 98.56 ppm, respectively. According to the results of linkage analysis and the literature,^{48,49} the intense peaks at 106.81, 81.75, 79.01, 83.11, and 67.62 ppm were assigned to C1, C2, C3, C4, and C5 of α -(1→5)-Araf, respectively, which confirmed the prominence of an arabinan-like structure as a side chain. The pectic polysaccharides of the rhamnogalacturonan I class were reported to consist of repeating units →2)- α -L-Rhap-(1→4)- α -D-GalpA-(1→ as backbone with side chains of either arabinan (average of 25–30 arabinose units) or galactooliosaccharides (average of 3–4 galactose units) attached to the O-4 position of →2)- α -L-Rhap-(1→ residues in the backbone.⁵⁰ On the basis of previous literature on the structure of pectic polysaccharides,^{11,51,52} the results of methylation and NMR analysis indicated the proposed partial structure of APPS (Figure 4), which was mainly consistent with previous partial characterization of alfalfa pectic polysaccharide indicating large amounts of D-galacturonic acid and 2-O-(α -D-galactopyranosyluronic acid)-L-rhamnose based on partial acid hydrolysis and/or partial acetolysis analysis.⁵ The primary difference between APPS and the previous arabinogalactorhamnoglycan type pectin was the degree of polymerization of the side chains.

Microscopic Morphology of APPS. TEM analysis was performed to observe the microstructure of APPS intuitively. As demonstrated in Figure 5, linear chains with minor branched structures were observed in APPS molecules under the experimental condition. The result was in agreement with that of methylation and NMR analyses that branching structure existed in APPS molecules.

Thermal Decomposition Analysis. Along with the structural properties, thermal decomposition characteristics also play an important role in the evaluation of polysaccharide applicability. In the present study, the thermal properties of APPS were assessed by thermogravimetry (TG), derivative thermogravimetry (DTG), and D²TG (second-time derivatives). From the TG curves, two steps of weight loss were observed during three different heating rates (Figure 6A). In the first step, a small amount of weight loss (~8%) occurred in the temperature range of 50–150 °C due to the loss of trapped water.⁵³ However, the structure of APPS was mainly pyrolyzed at the heating process of 200–400 °C, which resulted in ~55% weight loss. Thereby, the weight at 150 °C was designated 100% dry weight of APPS for the degradation analysis.

The curves of TG, DTG, and D²TG among three heating rates (β) were employed to calculate the thermal decomposition parameters of APPS in the 150–600 °C range (Figure 6B). Afterward, the pyrolysis properties of APPS were obtained from the β value of 0, which was deduced from each of the

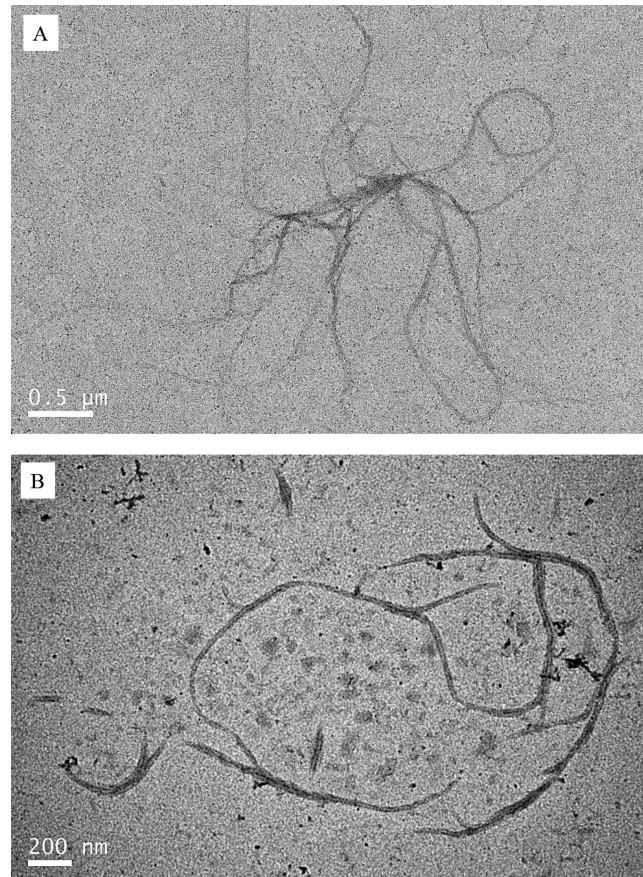


Figure 5. TEM images of APPS in sodium dodecyl sulfate (SDS) solution.

three temperatures (Figure 6C). Table 2 indicates the temperature of onset, maximum, and shift decomposition (T_o , T_p , and T_s) of APPS and their corresponding weight loss percentages (WL_o , WL_p , and WL_s). The decomposition of APPS was primarily started at 215.6 °C (T_o) and reached the maximum rate at 256.7 °C (T_p) with a loss of 12.80% dry weight (WL_p), whereas APPS experienced a rapid degradation in a narrow temperature range from the transition of 256.7 °C (T_p) to 328.0 °C (T_s). The major dry weight (51.12%) of APPS was lost in a 112.4 °C range of the heating process.

As shown in Figure 6D, the linear relationship and the fitted lines are nearly parallel in the conversion rate range of 0.3–0.7, which indicates approximate activation energies at different conversions and consequently implies the possibility of a single-reaction mechanism (or the unification of multiple-reaction mechanisms). However, the reaction mechanism could be different in the ranges of lower and higher conversion periods due to unsatisfied parallel lines at $\alpha < 0.3$ and $\alpha > 0.7$. The apparent activation energy (E_a) was thereby calculated to be 226.5 kJ/mol as listed in Table S2 in the Supporting Information, which was based on the FWO method at a conversion range from 0.3 to 0.7 with 0.1 increment (Figure 6D). The experimental pre-exponential factor (A) was obtained by the compensation effect relationship as eq 3 (Table S3). The compensation parameters of a and b were obtained from a plot of $\ln A$ versus E_a using the Coats–Redfern equation (eq 4) (Figure S4).

The major decomposition occurred in temperature range of 215.6–328.0 °C (Figure 6A), which could be caused by the

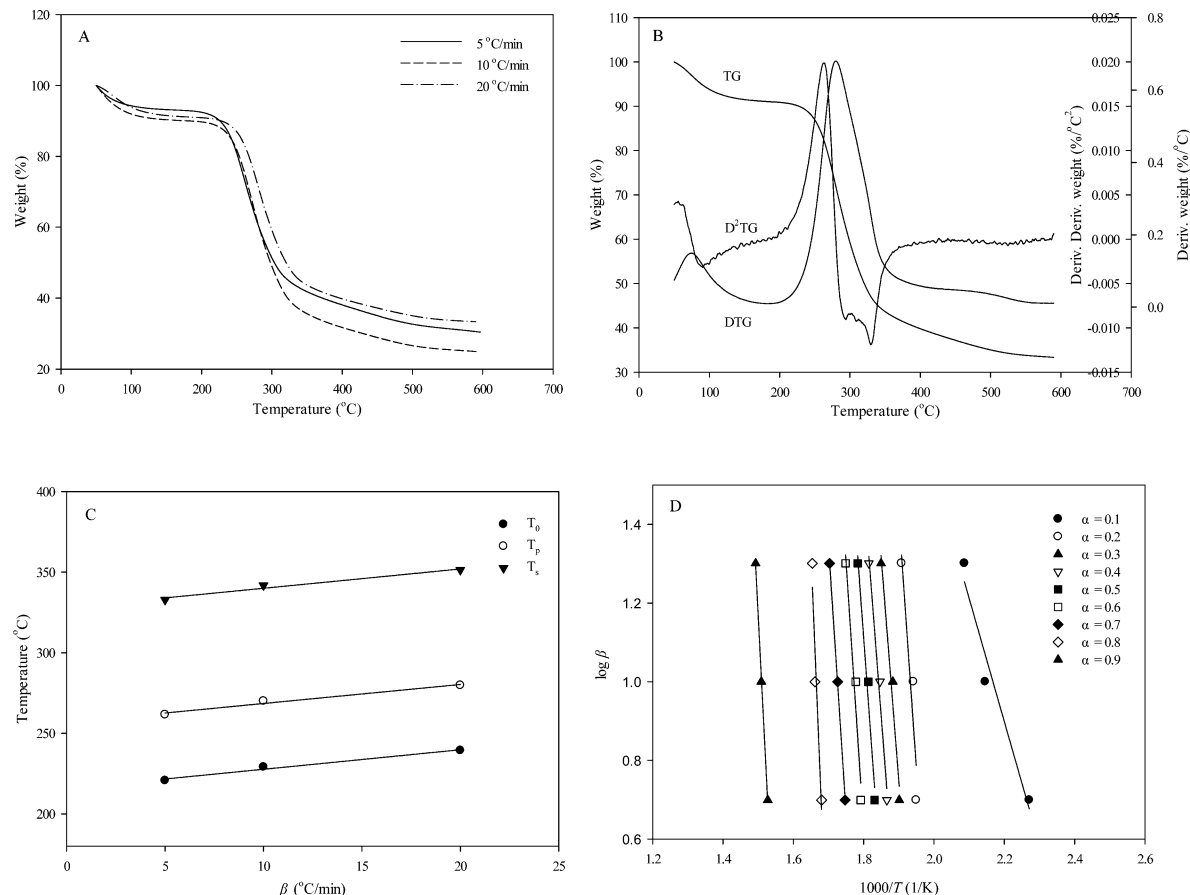


Figure 6. Thermal decomposition analysis of APPS: (A) TG curves of APPS at different heating rates; (B) determination of thermal decomposition parameters of APPS at a heating rate of 5 °C/min; (C) thermal degradation characteristics of APPS at different heating rates; (D) typical isoconversional plot of FWO method at different conversion rates.

Table 2. Thermal Degradation Characteristics of APPS^a

sample	$T_o \beta \rightarrow 0$ (°C)	WL _o (%)	$T_p \beta \rightarrow 0$ (°C)	WL _p (%)	$T_s \beta \rightarrow 0$ (°C)	WL _s (%)	$T_s - T_o$ (°C)	WL _s - WL _o (%)
APPS	215.6	1.43	256.7	12.80	328.0	52.55	112.4	51.12

^aData are the mean temperatures from three different heating rates. T = temperature, WL = weight loss, subscript: o = onset, p = DTG peak, s = shift, $\beta \rightarrow 0$ = extrapolated values to the heating rate of 0 °C/min.

degradation of polysaccharide structure.²⁰ Moreover, the E_a value of APPS was determined to be 226.5 kJ/mol, which revealed the good thermal stability of this pectic polysaccharide. The apparent activation energy (E_a) and pre-exponential factor (A) are the important parameters of the Arrhenius equation, where E_a might indicate a minimum energy requirement to initiate the decomposition reaction. These thermal decomposition characteristics are very important for the evaluation of the thermal stability of polysaccharides in their further application.

Anti-Inflammation Effects of APPS. The anti-inflammatory bioactivity of APPS was evaluated by determining its suppression effect of the IL-1 β , IL-6, and COX-2 mRNA expressions in RAW 264.7 macrophage cells stimulated by LPS. As shown in Figure 7, the greater concentration of APPS was associated with a stronger suppression for IL-1 β and IL-6 mRNA expressions, whereas increasing APPS concentration from 10 to 50 μ g/mL increased the COX-2 mRNA expression. The results indicated the potential application of APPS in food and medicine fields to reduce the risk of chronic inflammatory diseases.

In summary, a pectic polysaccharide (APPS) was purified from the hot alkali extract of alfalfa stems and characterized for its chemical and molecular structures. APPS was composed of repeating units of $\rightarrow 2$)- α -L-Rhap-(1 \rightarrow 4)- α -D-GalpA-(1 \rightarrow as the backbone and substituted at C-4 of Rhap with L-arabinosyl and D-galactosyl side chains, with a degree of branching value of 12%. The thermal stability and decomposition properties of APPS revealed the primary decomposition temperature range of 215.6–328.0 °C with an apparent activation energy (E_a) and a pre-exponential factor (A) of 226.5 kJ/mol and 2.10×10^{25} /s, respectively. APPS also showed a significant anti-inflammatory effect on LPS-stimulated RAW 264.7 mouse macrophage cells for suppression of IL-1 β , IL-6, and COX-2 gene expressions. Compared with previous studies of alfalfa pectin,⁵ the molecular structure of APPS was identified in combination with chemical characterization and morphological observation for the first time. The anti-inflammatory effect was also performed on a purified alfalfa pectic polysaccharide using an in vitro model. In addition, APPS showed a stronger potential anti-inflammatory effect compared with the pectic polysaccharide isolated from celery stalks.⁵⁴ Moreover, thermal degradation

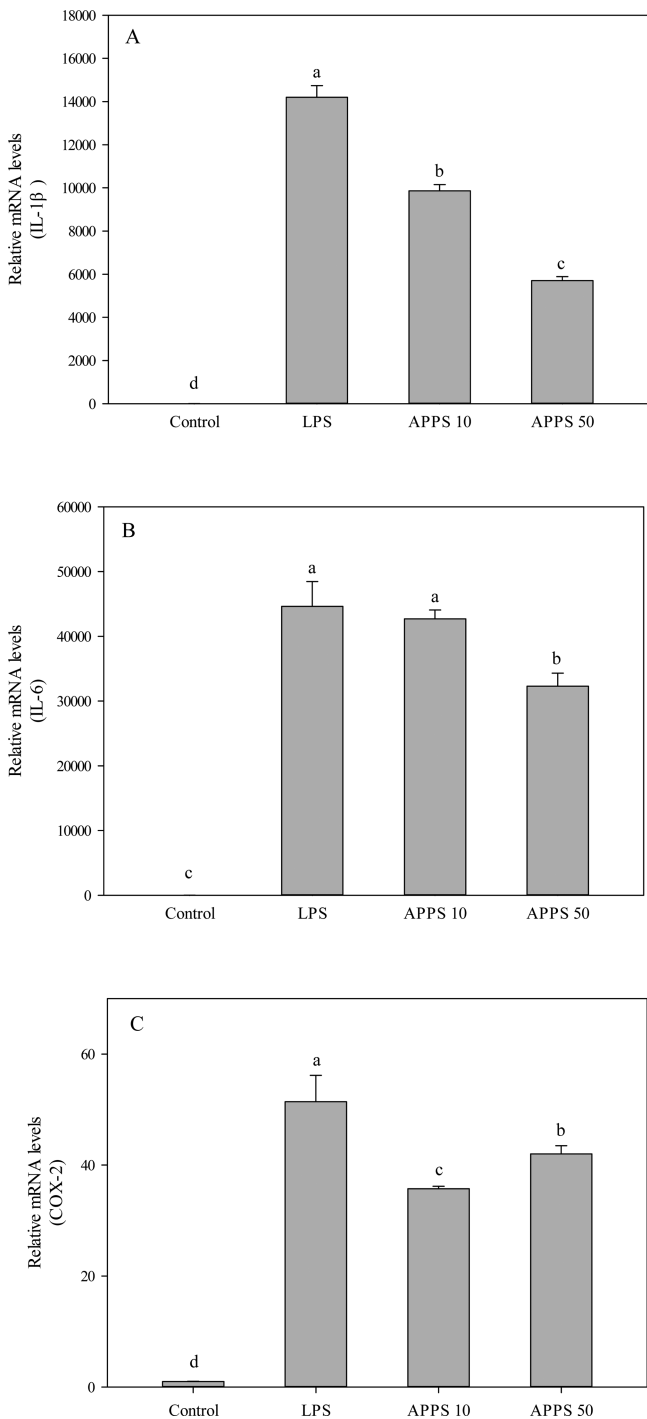


Figure 7. Effects of APPS on (A) IL-1 β , (B) IL-6, and (C) COX-2 mRNA expressions in LPS-stimulated RAW 264.7 mouse macrophage cells. LPS represents cells treated with LPS at a final concentration of 10 ng/mL; APPS 10 and APPS 50 stand for the final treatment concentrations of APPS at 10 and 50 μ g/mL followed by LPS inducement, respectively. The vertical bars represent the standard deviation ($n = 3$) of each data point. Different letters (a–d) represent significant differences ($P < 0.05$).

behavior was estimated to illustrate the stability for pectic polysaccharides from alfalfa for the first time. These results indicated the potential application of APPS in functional foods and dietary supplement products.

ASSOCIATED CONTENT

Supporting Information

Tables S1–S3 and Figures S1–S4. This material is available free of charge via the Internet at <http://pubs.acs.org>.

AUTHOR INFORMATION

Corresponding Author

* (L.Y.) Phone: (301) 405-0761. E-mail: lyu5@umd.edu.

Funding

This project was supported by a General Grant from the China Postdoctoral Science Foundation (Grant 2014M561476), a special fund for Agro-scientific Research in the Public Interest (Grant 201203069), a National High Technology Research and Development Program of China (Grants 2013AA102202 and 2013AA102207), SJTU 985-III disciplines platform and talent fund (Grants TS0414115001 and TS0320215001), and a grant from Wilmar (Shanghai) Biotechnology Research & Development Center Co., Ltd.

Notes

The authors declare no competing financial interest.

REFERENCES

- (1) Hu, Y. G.; Cash, D. Global status and development trends of alfalfa. In *Alfalfa Management Guide for Ningxia*; Cash, D., Ed.; FAO: Rome, Italy, 2009; pp 1–3.
- (2) Lamb, J. F. S.; Jung, H. J. G.; Sheaffer, C. C.; Samac, D. A. Alfalfa leaf protein and stem cell wall polysaccharide yields under hay and biomass management systems. *Crop Sci.* **2007**, *47*, 1407–1415.
- (3) Aspinall, G. O.; McGrath, D. Hemicelluloses of lucerne. *J. Chem. Soc. C* **1966**, 2133–2139.
- (4) Aspinall, G. O.; Fanshawe, R. S. Pectic substances from lucerne (*Medicago sativa*). Part I. Pectic acid. *J. Chem. Soc.* **1961**, 4215–4225.
- (5) Aspinall, G. O.; Gestetner, B.; Molloy, J. A.; Uddin, M. Pectic substances from lucerne (*Medicago sativa*). Part II. Acidic oligosaccharides from partial hydrolysis of leaf and stem pectic acids. *J. Chem. Soc. C* **1968**, 2554–2559.
- (6) Wang, S. P.; Dong, X. F.; Tong, J. M. Optimization of enzyme-assisted extraction of polysaccharides from alfalfa and its antioxidant activity. *Int. J. Biol. Macromol.* **2013**, *62*, 387–396.
- (7) Dong, X. F.; Gao, W. W.; Su, J. L.; Tong, J. M.; Zhang, Q. Effects of dietary polysavone (alfalfa extract) and chlortetracycline supplementation on antioxidation and meat quality in broiler chickens. *Br. Poult. Sci.* **2011**, *52*, 302–309.
- (8) Dong, X. F.; Gao, W. W.; Tong, J. M.; Jia, H. Q.; Sa, R. N.; Zhang, Q. Effect of polysavone (alfalfa extract) on abdominal fat deposition and immunity in broiler chickens. *Poult. Sci.* **2007**, *86*, 1955–1959.
- (9) Voragen, A. J.; Coenen, G.; Verhoef, R.; Schols, H. Pectin, a versatile polysaccharide present in plant cell walls. *Struct. Chem.* **2009**, *20*, 263–275.
- (10) Sila, D. N.; Van Buggenhout, S.; Duvetter, T.; Fraeye, I.; De Roeck, A.; Van Loey, A.; Hendrickx, M. Pectins in processed fruits and vegetables: Part II. Structure-function relationships. *Compr. Rev. Food Sci. Food Saf.* **2009**, *8*, 86–104.
- (11) Dong, Q.; Liu, X.; Yao, J.; Dong, X.; Ma, C.; Xu, Y.; Fang, J.; Ding, K. Structural characterization of a pectic polysaccharide from *Nerium indicum* flowers. *Phytochemistry* **2010**, *71*, 1430–1437.
- (12) Caffall, K. H.; Mohnen, D. The structure, function, and biosynthesis of plant cell wall pectic polysaccharides. *Carbohydr. Res.* **2009**, *344*, 1879–1900.
- (13) Duan, J. Y.; Chen, V. L.; Dong, Q.; Ding, K.; Fang, J. L. Chemical structure and immunoinhibitory activity of a pectic polysaccharide containing glucuronic acid from the leaves of *Diospyros kaki*. *Int. J. Biol. Macromol.* **2010**, *46*, 465–470.

- (14) Habibi, Y.; Heyraud, A.; Mahrouz, M.; Vignon, M. R. Structural features of pectic polysaccharides from the skin of *Opuntia ficus-indica* prickly pear fruits. *Carbohydr. Res.* **2004**, *339*, 1119–1127.
- (15) Novosel'Skaya, I. L.; Voropaeva, N. L.; Semenova, L. N.; Rashidova, S. S. Trends in the science and applications of pectins. *Chem. Nat. Compd.* **2000**, *36*, 1–10.
- (16) Vincken, J. P.; Schols, H. A.; Oomen, R. J. F. J.; McCann, M. C.; Ulvskov, P.; Voragen, A. G. J.; Visser, R. G. F. If homogalacturonan were a side chain of rhamnogalacturonan I. Implications for cell wall architecture. *Plant Physiol.* **2003**, *132*, 1781–1789.
- (17) Fraeye, I.; Deroeck, A.; Duvetter, T.; Verlent, I.; Hendrickx, M.; Vanloey, A. Influence of pectin properties and processing conditions on thermal pectin degradation. *Food Chem.* **2007**, *105*, 555–563.
- (18) Smout, C.; Sila, D. N.; Vu, T. S.; Van Loey, A. M. L.; Hendrickx, M. E. G. Effect of preheating and calcium pre-treatment on pectin structure and thermal texture degradation: a case study on carrots. *J. Food Eng.* **2005**, *67*, 419–425.
- (19) Iqbal, M. S.; Massey, S.; Akbar, J.; Ashraf, C. M.; Masih, R. Thermal analysis of some natural polysaccharide materials by isoconversional method. *Food Chem.* **2013**, *140*, 178–182.
- (20) Yao, F.; Wu, Q. L.; Lei, Y.; Guo, W. H.; Xu, Y. J. Thermal decomposition kinetics of natural fibers: activation energy with dynamic thermogravimetric analysis. *Polym. Degrad. Stab.* **2008**, *93*, 90–98.
- (21) Liu, X. X.; Yu, L.; Liu, H. S.; Chen, L.; Li, L. Thermal decomposition of corn starch with different amylose/amyllopectin ratios in open and sealed systems. *Cereal Chem.* **2009**, *86*, 383–385.
- (22) Santos, J. C. O.; Santos, I. M. G.; Souza, A. G.; Prasad, S.; Santos, A. V. Thermal stability and kinetic study on thermal decomposition of commercial edible oils by thermogravimetry. *J. Food Sci.* **2002**, *67*, 1393–1398.
- (23) De Wit, J. N. Thermal stability and functionality of whey proteins. *J. Dairy Sci.* **1990**, *73*, 3602–3612.
- (24) Kapu Niak, J.; Ciesielski, W.; Kozio, J. J.; Tomasik, P. Thermogravimetry- and differential scanning calorimetry-based studies of the solid state reactions of starch polysaccharides with proteogenic amino acids. *Thermochim. Acta* **2001**, *372*, 119–128.
- (25) Dollinger, G.; Cunico, B.; Kunitani, M.; Johnson, D.; Jones, R. Practical on-line determination of biopolymer molecular weights by high-performance liquid chromatography with classical light-scattering detection. *J. Chromatogr., A* **1992**, *592*, 215–228.
- (26) Hill, H. D.; Straka, J. G. Protein determination using bicinchoninic acid in the presence of sulphydryl reagents. *Anal. Biochem.* **1988**, *170*, 203–208.
- (27) DuBois, M.; Gilles, K. A.; Hamilton, J. K.; Rebers, P. A.; Smith, F. Colorimetric method for determination of sugars and related substances. *Anal. Chem.* **1956**, *28*, 350–356.
- (28) Blumenkrantz, N.; Asboe-Hansen, G. New method for quantitative determination of uronic acids. *Anal. Biochem.* **1973**, *54*, 484–489.
- (29) Yan, W.; Niu, Y. G.; Lv, J. L.; Xie, Z. H.; Jin, L.; Yao, W. B.; Gao, X. D.; Yu, L. L. L. Characterization of a heteropolysaccharide isolated from diploid *Gynostemma pentaphyllum* Makino. *Carbohydr. Polym.* **2013**, *92*, 2111–2117.
- (30) Pettolino, F. A.; Walsh, C.; Fincher, G. B.; Bacic, A. Determining the polysaccharide composition of plant cell walls. *Nat. Protoc.* **2012**, *7*, 1590–1607.
- (31) Kim, J. S.; Reuhs, B. L.; Michon, F.; Kaiser, R. E.; Arumugham, R. G. Addition of glycerol for improved methylation linkage analysis of polysaccharides. *Carbohydr. Res.* **2006**, *341*, 1061–1064.
- (32) CCRC. <http://www.ccrc.uga.edu/specdb/ms/pmaa/pframe.html> (accessed Oct 15, 2014).
- (33) Rezanka, T.; Sigler, K. Structural analysis of a polysaccharide from *Chlorella kessleri* by means of gas chromatography-mass spectrometry of its saccharide alditols. *Folia Microbiol. (Praha)* **2007**, *52*, 246–252.
- (34) Chen, L.; Cheung, P. C. K. Mushroom dietary fiber from the fruiting body of *Pleurotus tuber-regium*: fractionation and structural elucidation of nondigestible cell wall components. *J. Agric. Food Chem.* **2014**, *62*, 2891–2899.
- (35) Liu, X. X.; Ma, H. X.; Yu, L.; Chen, L.; Tong, Z.; Chen, P. Thermal-oxidative degradation of high-amylose corn starch. *J. Therm. Anal. Calorim.* **2014**, *115*, 659–665.
- (36) Flynn, J. H.; Wall, L. A. General treatment of the thermogravimetry of polymers. *J. Res. Natl. Bur. Stand.* **1966**, *70*, 487–523.
- (37) Ozawa, T. A new method of analyzing thermogravimetric data. *Bull. Chem. Soc. Jpn.* **1965**, *38*, 1881–1886.
- (38) Zhang, X. W.; Shang, P. P.; Qin, F.; Zhou, Q.; Gao, B. Y.; Huang, H. Q.; Yang, H. S.; Shi, H. M.; Yu, L. L. L. Chemical composition and antioxidative and anti-inflammatory properties of ten commercial mung bean samples. *LWT—Food Sci. Technol.* **2013**, *54*, 171–178.
- (39) Huang, H. Q.; Cheng, Z. H.; Shi, H. M.; Xin, W. B.; Wang, T. T. Y.; Yu, L. L. L. Isolation and characterization of two flavonoids, engeletin and astilbin, from the leaves of *Engelhardia roxburghiana* and their potential anti-inflammatory properties. *J. Agric. Food Chem.* **2011**, *59*, 4562–4569.
- (40) Casassa, E. F.; Markovitz, H. Statistical thermodynamics of polymer solutions. I. Theory of the second virial coefficient for a homogeneous solute. *J. Chem. Phys.* **1958**, *29*, 493–503.
- (41) Hawker, C. J.; Lee, R.; Frechet, J. M. J. One-step synthesis of hyperbranched dendritic polyesters. *J. Am. Chem. Soc.* **1991**, *113*, 4583–4588.
- (42) Ridley, B. L.; O'Neill, M. A.; Mohnen, D. Pectins: structure, biosynthesis, and oligogalacturonide-related signaling. *Phytochemistry* **2001**, *57*, 929–967.
- (43) Èopíková, J.; Synytsya, A.; Èerná, M.; Kaasová, J.; Novotná, M. Application of FT-IR spectroscopy in detection of food hydrocolloids in confectionery jellies and food supplements. *Czech J. Food Sci.* **2000**, *19*, 51–56.
- (44) Kac Uráková, M.; Čapek, P.; Sasinková, V.; Wellner, N.; Ebringerová, A. FT-IR study of plant cell wall model compounds: pectic polysaccharides and hemicelluloses. *Carbohydr. Polym.* **2000**, *43*, 195–203.
- (45) Ryden, P.; Colquhoun, I. J.; Selvendran, R. R. Investigation of structural features of the pectic polysaccharides of onion by ¹³C-n.m.r. spectroscopy. *Carbohydr. Res.* **1989**, *185*, 233–237.
- (46) Keenan, M. H. J.; Belton, P. S.; Matthew, J. A.; Howson, S. J. A ¹³C-n.m.r. study of sugar-beet pectin. *Carbohydr. Res.* **1985**, *138*, 168–170.
- (47) Joseleau, J.; Chambat, G.; Vignon, M.; Barnoud, F. Chemical and ¹³C N.M.R. studies on two arabinans from the inner bark of young stems of *Rosa glauca*. *Carbohydr. Res.* **1977**, *58*, 165–175.
- (48) Dourado, F.; Cardoso, S.; Silva, A.; Gama, F.; Coimbra, M. NMR structural elucidation of the arabinan from *Prunus dulcis* immunobiological active pectic polysaccharides. *Carbohydr. Polym.* **2006**, *66*, 27–33.
- (49) Cardoso, S. M.; Silva, A. M.; Coimbra, M. A. Structural characterisation of the olive pomace pectic polysaccharide arabinan side chains. *Carbohydr. Res.* **2002**, *337*, 917–924.
- (50) Willats, W. T.; McCartney, L.; Mackie, W.; Knox, J. P. Pectin: cell biology and prospects for functional analysis. In *Plant Cell Walls*; Carpita, N. C., Campbell, M., Tierney, M., Eds.; Springer: Dordrecht, The Netherlands, 2001; pp 9–27.
- (51) Zheng, Y.; Mort, A. Isolation and structural characterization of a novel oligosaccharide from the rhamnogalacturonan of *Gossypium hirsutum* L. *Carbohydr. Res.* **2008**, *343*, 1041–1049.
- (52) Habibi, Y.; Mahrouz, M.; Vignon, M. R. Arabinan-rich polysaccharides isolated and characterized from the endosperm of the seed of *Opuntia ficus-indica* prickly pear fruits. *Carbohydr. Polym.* **2005**, *60*, 319–329.
- (53) Iqbal, M. S.; Akbar, J.; Saghir, S.; Karim, A.; Koschella, A.; Heinze, T.; Sher, M. Thermal studies of plant carbohydrate polymer hydrogels. *Carbohydr. Polym.* **2011**, *86*, 1775–1783.
- (54) Ovodova, R. G.; Golovchenko, V. V.; Popov, S. V.; Popova, G. Y.; Paderin, N. M.; Shashkov, A. S.; Ovodov, Y. S. Chemical

composition and anti-inflammatory activity of pectic polysaccharide isolated from celery stalks. *Food Chem.* **2009**, *114*, 610–615.